AC Conductivity and Dielectric properties of the $Cd_{0.4}Mn_{0.6}Co_xFe_{2-x}O_4$ ferrite system

T. M. Meaz*[*a], M. A. Amer[a], M. A. Elkestawy[b], and A. I. Ghoneim .

[a]Physics Department, Faculty of Science, Tanta University, Tanta, Egypt.
[b]Physics Department, Faculty of Science, Suez Canal University, Suez, Egypt.
[*]tmeaz@yahoo.com

A series of polycrystalline spinel ferrites with the composition $Cd_{0.4}Mn_{0.6}Co_xFe_{2-x}O_4$, (x=0.00, 0.125, 0.25, 0.375, 0.5, 0.75, and 1.00) were prepared by the standard ceramic method to study the effect of Co^{3+} ions substitution on their AC electrical conductivity and dielectric properties at different frequencies and temperatures. It was found that the electrical conductivity decreases as Co^{3+} ions substitution increases. The results obtained reveal a semiconductor behavior of these samples. Dielectric constant and dielectric loss were explained with the aid of Maxwell-Wagner and Koop's model. The electrical conductivity was explained on the basis of the hopping conduction mechanism.

1. Introduction:

Spinel ferrites have many different applications from Microwave to radio frequency range. Several studies on the electrical properties for spinel ferrites have been reported [1-5]. Co, Mn-Cd ferrites usage in the field of microwave industry is influenced by their physical and chemical properties, which is in turn influenced by several factors such as method and conditions of preparation as well as the amount of additives. Co-ferrite has a very interesting properties where, the anisotropy of the Co ferrite can be used to compensate the negative anisotropies of other ferrites. Cobalt has been used to lower losses and for temperature compensation. Another advantage of cobalt is its ability to make the ferrite susceptible to magnetic annealing. Also, Co has high magnetic moment [6]. They are relatively inexpensive, stable, easily manufactured and widely used as both low- and high- frequency devices. The electrical and magnetic properties of many ferrites are found to change markedly by controlling the preparation conditions such as the firing temperature and additives [6].

2. Experimental Procedures:

$Cd_{0.4}Mn_{0.6}Co_xFe_{2-x}O_4$ with x= 0.00, 0.125, 0.25, 0.375, 0.5, 0.75 were prepared by standard ceramic technique [7]. The disk samples were polished to obtain uniform parallel surfaces. Finally the surfaces of the disks were Repolished and coated by a silver paste that acts as a good contact for electrical measurements. The AC conductivity and dielectric properties were measured at different temperatures using a complex impedance technique with low frequency Lock-in-Amplifier in the frequency range 10^2-10^5 Hz [7, 8, 9].

3. Results and discussions

3.1. AC conductivity (σ_{ac}')

Figure (1) illustrates the relation between the real part of ac conductivity (σ_{ac}') and the temperature (10^3/T) at: 1, 5, 10, 20, 50 and 100 KHz selected frequencies. At each frequency the ac conductivity increases continuously with increasing temperature, indicating a semiconducting behavior which is similar for all the studied samples. The ac conductivity is frequency dependent at constant temperature; the frequency dependence of ac conductivity decreases with increasing temperature. Below Curie temperature, two distinct regions with different were slopes observed. The rate it of increasing of σ_{ac}' with temperature at low temperatures (region I) is less than it at higher temperatures (region II). Fig. (2) represents the variation of the σ_{ac}' with frequency at different constant temperatures for all the investigated samples. It is evident that the frequency dependence dominates at low temperatures, where σ_{ac}' increases continuously with increasing frequency, the rate of this increase decreases with increasing temperature. At high temperatures, σ_{ac}' becomes almost frequency independent and the dc contribution becomes significant.

The σ_{ac}' results could be explained by [9-13]:

$$\sigma_{Total} = \sigma_{dc} + \sigma_{ac}$$

where σ_{dc}(T) is dc conductivity which is temperature dependent, and the σ_{ac} is the ac conductivity which is temperature dependent. Thus σ_{ac} is related to the frequency and temperature by the relation [9, 11-14]:

$$\sigma_{ac} = B\omega^S \qquad (1)$$

where $\omega = 2\pi f$ is the angular frequency, B is a constant has the conductivity units and $\boldsymbol{S}$ is the frequency exponent dimensionless parameter, which is temperature dependent and takes the values from zero to one. B and S are composition and temperature dependent parameters [14]. Frequency and temperature dependent conductivity σ_{ac} was calculated at different frequencies and different temperatures using equation (1).

Figure (3) show straight lines illustrating the relation between log σ_{ac} and log ω at different temperatures. The slopes of these lines give the frequency exponent ***S*** at each temperature. Fig. (3) show that σ_{ac} increases with increasing the angular frequency (ω) at low temperatures, while it becomes almost frequency independent at high temperatures. A similar behavior was observed before for many ferrite systems [3-5]. The effect of temperature on the frequency exponent parameter ***S*** is illustrated in figure (4). For the first five samples where $0.0 \leq x \leq 0.5$ at low temperatures, T<470 K, the frequency exponent ***S*** decreases rapidly, and above this temperature it decreases slowly. For x=0.75 and x=1.00 it decreases rapidly then goes to a minimum and after which it increases.

It is well known that the dependence of ***S*** on ***T*** and ***ω*** reveals the mechanism of conduction [9]. Qualitatively, small polaron conductivity[9] are usually characterized by an increase in ***S*** as temperature increases, while correlated barrier hopping[9] for instance shows a decrease in ***S*** with increasing temperature which is the dominant in the first five samples where $0.0 \leq x \leq 0.5$. On the other hand; for quantum mechanical tunneling, ***S*** is independent on temperature, while large overlap polaron [9] conductivity is associated with a decrease of ***S*** reaching a minimum followed by increase in ***S*** with the temperature which is the dominant in the last two samples where x=0.75 and 1.00. According to the behavior of ***S*** in figure (4), it was find that the two mechanisms may contribute to the ac conductivity in the investigated samples. The first mechanism at relatively low temperature is the correlated barrier hopping. The second mechanism suggested to predominate at higher temperatures is the large overlap polaron. As a conclusion it is found that: I- the correlated barrier hopping is the predominant conduct mechanism in the first five samples ($0.00 \leq x \leq 0.5$). II- the large overlap polaron is the predominant in the last two samples (x=0.75 and 1.00) [9].

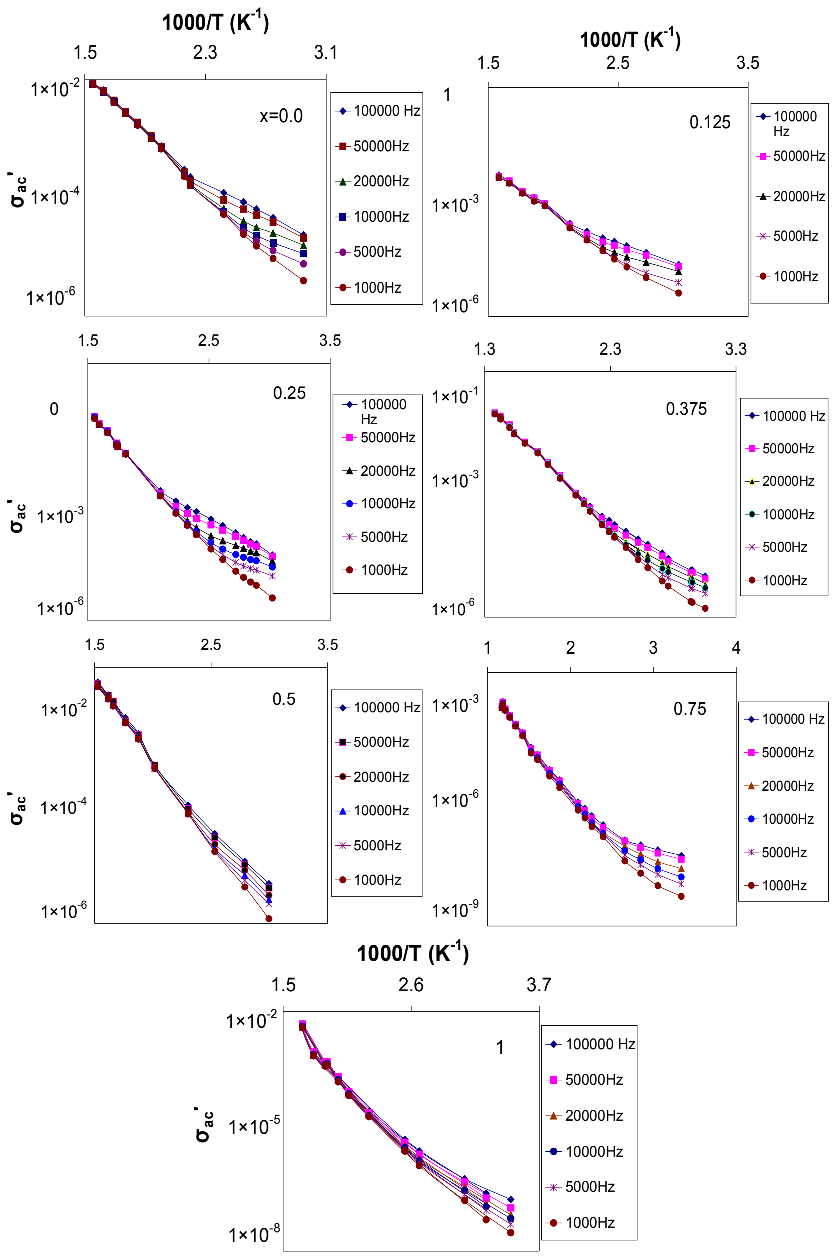

Fig. (1) : Temperature dependence of the real part of ac conductivity σ_{ac}' for the investigated samples at some selected frequencies.

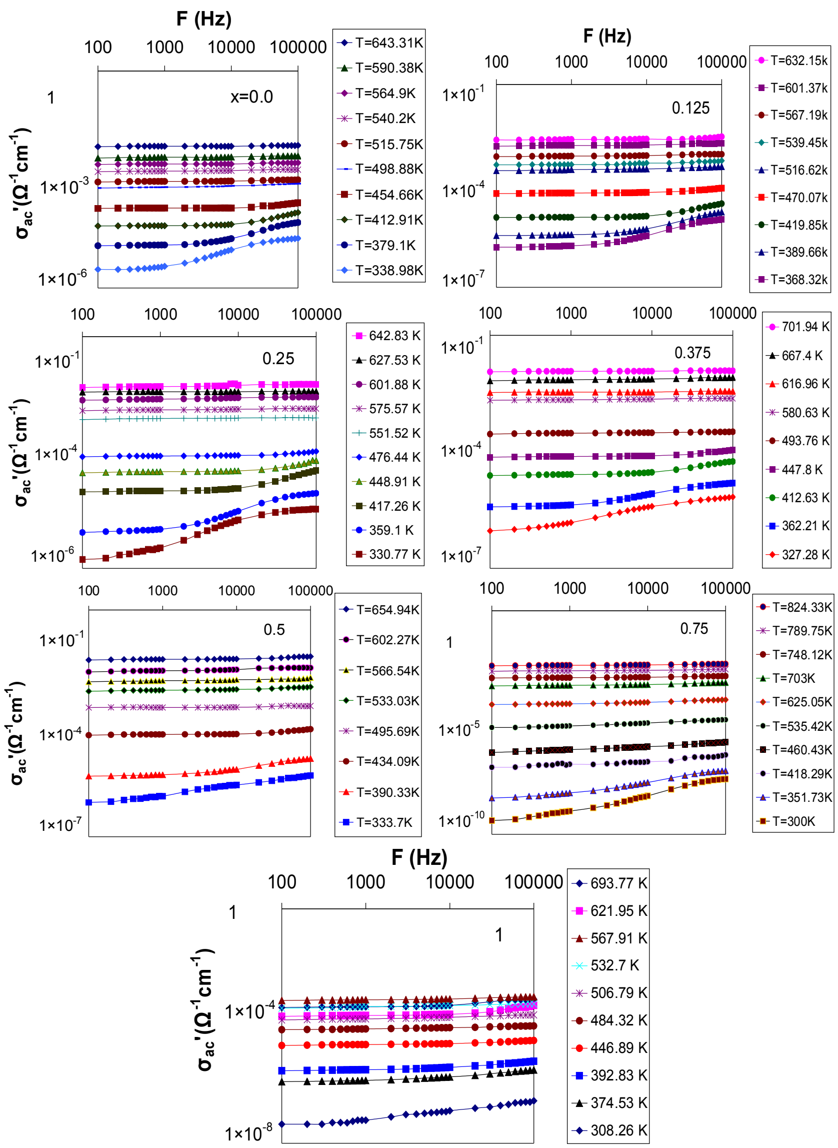

Fig. (2) : frequency dependence of the real part of ac conductivity σ_{ac}' for the investigated samples at different temperatures.

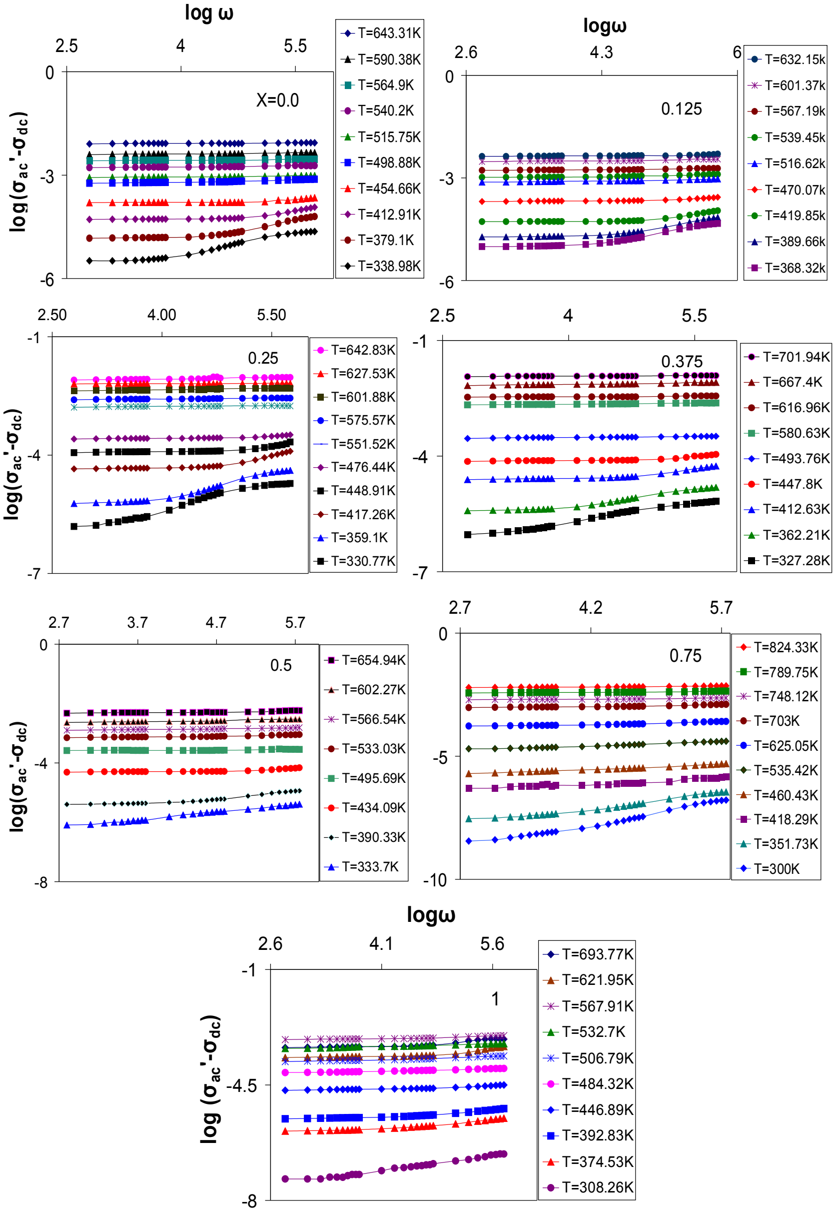

Fig. (3) : Frequency dependence part of ac conductivity σ_2 versus angular frequency for the investigated samples at different temperatures.

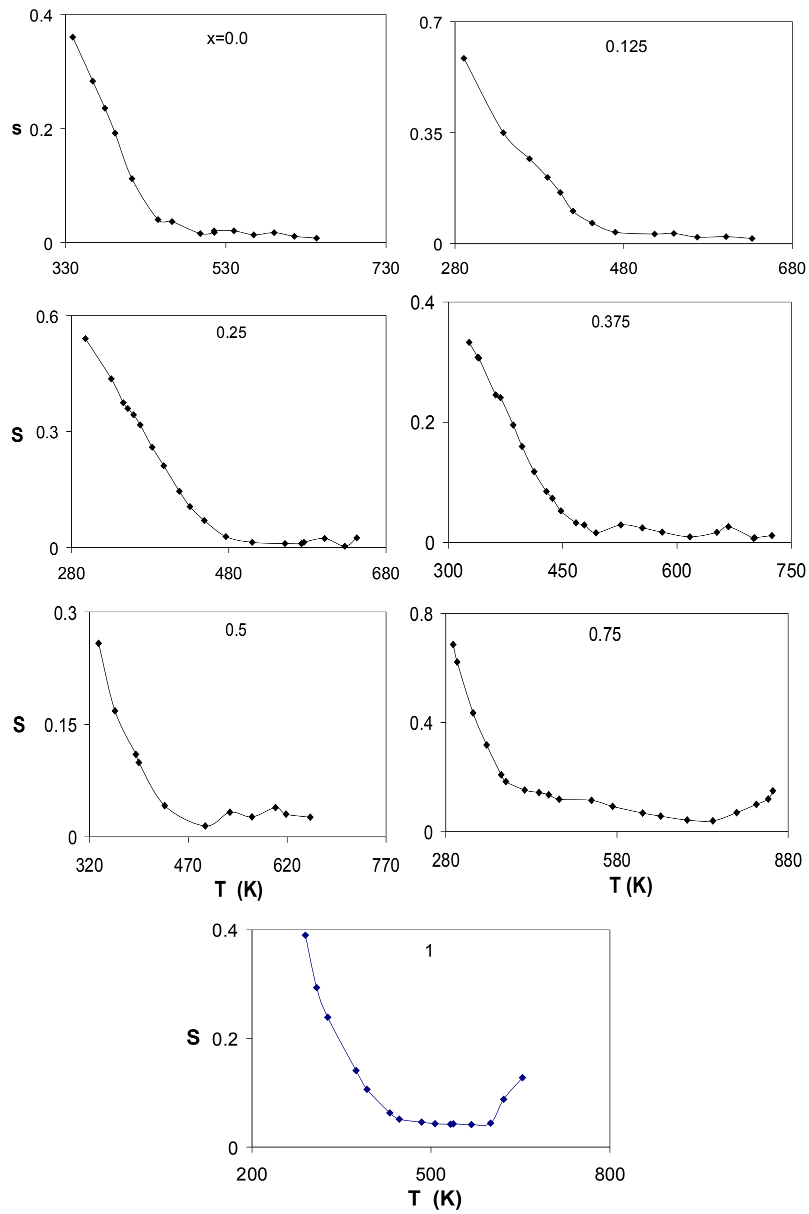

Fig. (4) : Temperature dependence of S for the investigated samples.

3.2. Dielectric Constant Behavior:

The variation of the dielectric constant **ε'** with frequency at some selected constant temperatures has been studied for all samples and it is shown in Fig. (5). A dispersion of **ε'** was observed for all samples. At low frequencies **ε'** values are high, and as the frequency increases **ε'** decreases. Moreover, **ε'** increases with increasing temperature. Several investigators have studied the frequency and temperature dependence of **ε'** in ferrites [14-20]. Generally, the dispersion of **ε'** can be explained on the basis of the space charge polarization due to the inhomogeneous dielectric structure as discussed by Maxwell-Wagner and Koop's model [15]. In this case the high observed values of **ε'** in the present samples at low frequencies can be explained with the aid of Koop's model. The ferrite sample is consisting of grains and grain boundaries. The resistivity of grain boundaries is larger than that of grains. This leads to the accumulation of charges at the interfaces between grains and grain boundaries. These charges contribute to the polarization and consequently to the dielectric constant **ε'** at low frequencies. Whereas, at high frequencies, such charges cannot follow the variation of the field and therefore their contribution to the polarization ceases.

The **ε'** increases gradually with increasing temperature at low frequencies, whereas at high frequencies the increase of **ε'** with increasing temperature is less. This behavior of **ε'** with temperature at low frequencies is due to the semiconductor behavior of the samples, whereas at high frequencies this property is obscured by the disability of charges at the boundaries to follow the variation of the field. This effect leads to decrease the dielectric constant with increasing frequency. Moreover, this indicates that the main contributor to the polarization process – interfacial polarization- and consequently the dielectric behavior in ferrites has a similar mechanism as that of the conduction process [21].

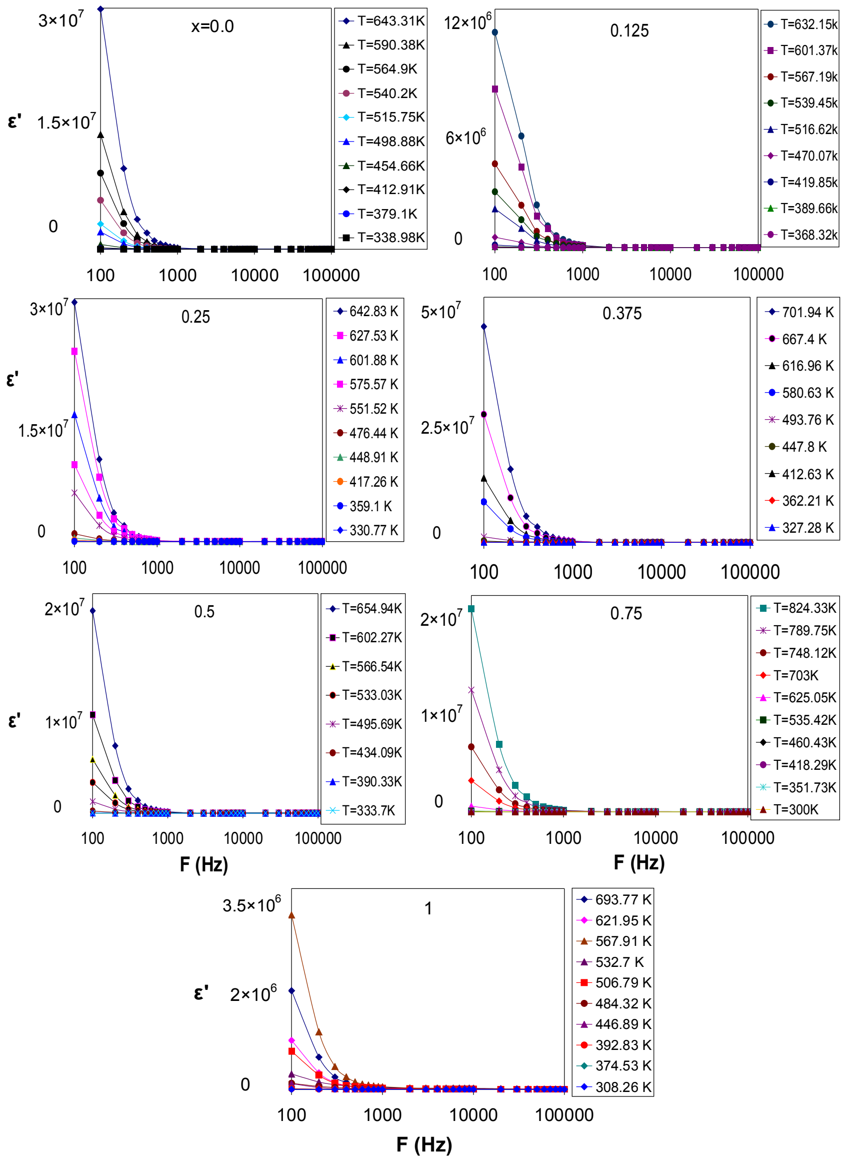

Fig. (5) : Frequency dependence of the dielectric constant ε' for the investigated samples at different temperatures.

3.3. Dielectric Loss Tangent Behavior:

Figure (6) shows the variation of the dielectric loss tangent tan δ with frequency at different constant temperatures for all the investigated samples. The relation of tan *δ* with frequency shows a relaxation spectrum with a loss peak at nearly the mid range of frequency. The presence of the loss peak in the relation of tan *δ* versus frequency can be interpreted in the light of the strong correlation between the conduction mechanism and the dielectric behavior in the spinel ferrites as pointed out by Iwauchi [22]. The conduction mechanism in the present compounds is explained in terms of hopping conduction process. In this case, a maximum in the dielectric loss tangent is observed when the hopping frequency of the hopping process is approximately equal to the frequency of the external electric field. The frequency dependence of tan *δ* at different constant temperatures clearly shows that as the temperature increases, the peaks are shifted towards higher frequency, while they are shifted towards higher frequencies with increasing temperature and Co substitution content. It can be noticed also that the height of the peak increases as temperature increases. The occurrence of the loss peaks in these compounds could be explained on the basis of the electrical interactions between cation–anion–cation occurred over the crystallographic sites in these compounds. Based on cation–anion–cation and cation–cation interactions over the octahedral B-site as pointed out by Goodenough, the relaxation process in $Cd_{0.4}Mn_{0.6}Co_xFe_{2-x}O_4$ compound can be attributed to the cation–anion–cation interactions over B-site which occurs between 3d-wave function of the transition element and 2p wave function of the oxygen as a result of the application of alternating electric field [21]. This interaction can be assigned as $[Fe^{3+}– O^{2–}– Fe^{3+}]$. Introduction of Co^{3+} with $(3d^{10})$ in place of Fe^{3+} at B-site in this unit cell will increase this interaction. Whereas Co ions prefer the octahedral B-site [23], as varying Co content, both electron hopping between Fe^{2+} and Fe^{3+} ions and hole exchange between Co^{3+} and Co^{2+} ions which are taking place at the octahedral B-site are responsible for electric conduction.

The shift of this maximum towards higher frequencies as temperature increases is often attributed to the increase of the hopping frequency of the charge carriers as the temperature increases.

Figure (7) illustrates the temperature dependence of tan δ at some selected constant frequencies. It can be seen that tan δ values show maxima shifted towards higher temperatures.

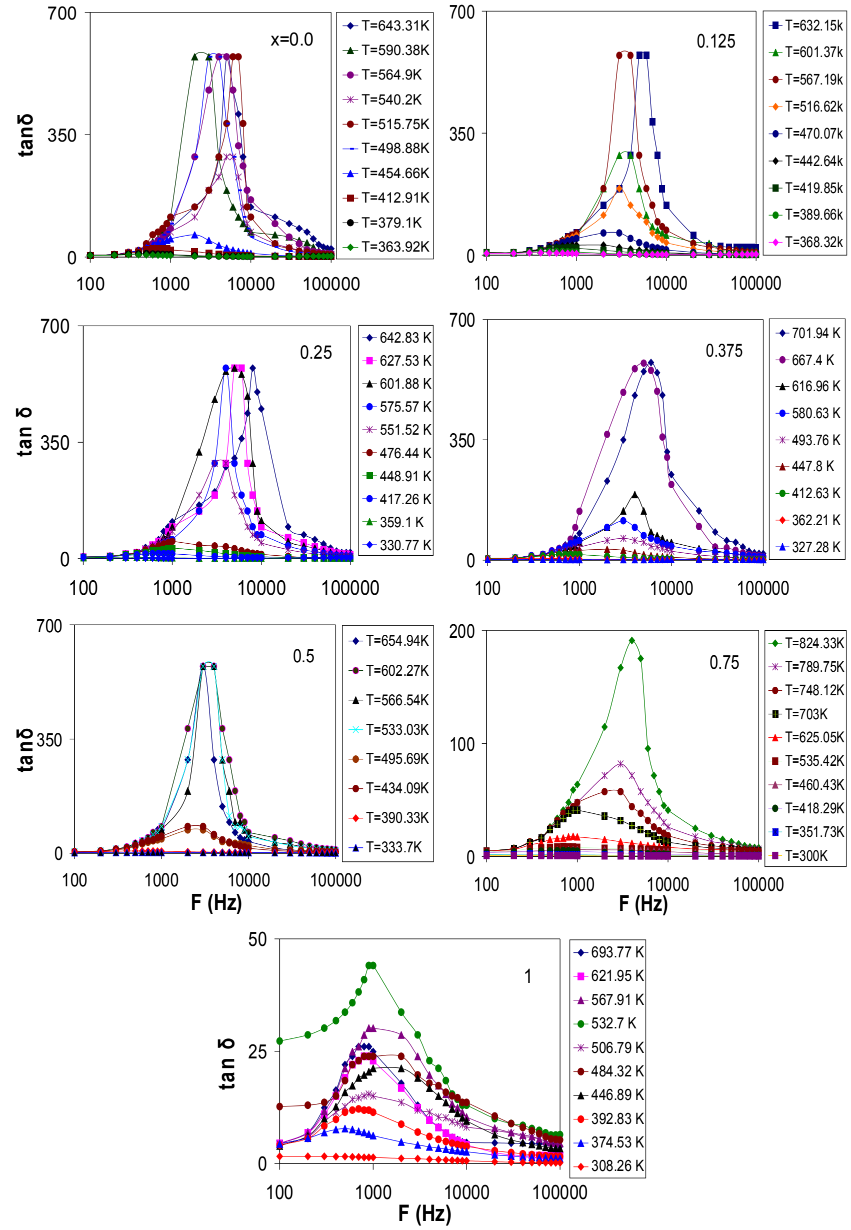

Fig. (6) : Frequency dependence of loss tangent tanδ at different temperatures for the investigated samples.

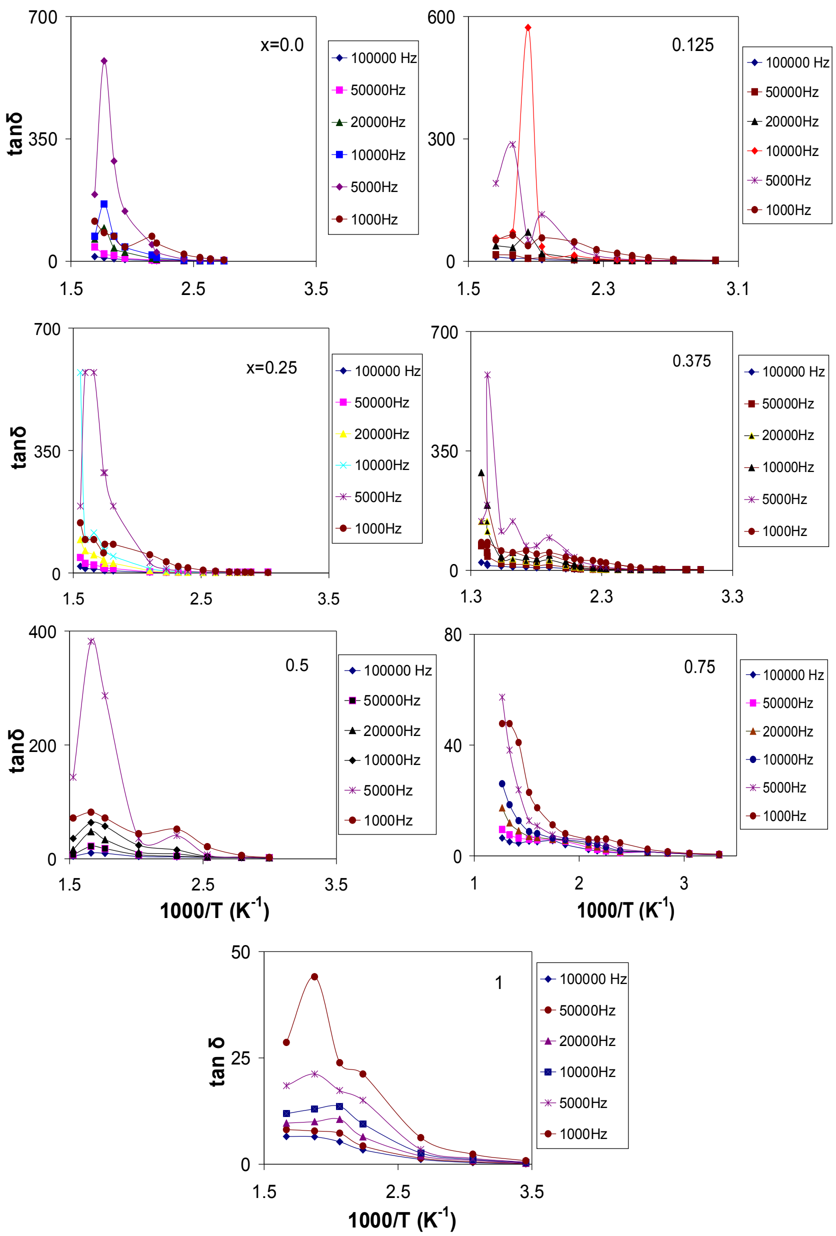

Fig. (7) : Temperature dependence of loss tangent tanδ for the investigated samples.

4. Conclusion:

From the above studies it can be concluded that:

The σ_{ac}' increases continuously with increasing temperature, indicating a semiconductor behavior for all samples. At high temperatures σ_{ac}' becomes almost frequency independent and the D. C. contribution becomes significant. Below Curie temperature, two distinct regions are observed in the plot of σ_{ac}' versus temperature.

Frequency and temperature dependent of conductivity σ_{ac}increases with increasing the angular frequency (ω) at low temperatures, while it becomes almost frequency independent at high temperatures. The slopes of the lines of log σ_{ac} versus temperature give the frequency exponent *S* at each temperature. From the plot of S versus T it is found that: a- the correlated barrier hopping is the predominant conduction mechanism in the first five samples ($0.00 \leq x \leq 0.5$). b- the large overlap polaron is the predominant conduction mechanism in the last two samples ($x = 0.75$ and 1.00).

A dispersion of the dielectric constant ε' is observed for all samples. At low frequencies ε' values are high, as the frequency increase ε' decreases, moreover, ε' increases with increasing temperature.

The relation of the dielectric loss tangent tan δ with frequency shows a relaxation spectrum with a loss peak at nearly the mid range of frequency. As the temperature increases, the peaks are shifted towards higher frequency.

References:

1. A.R. Shitre, V.B. Kawade, G.K. Bichile, K.M. Jadhav, *Mater. Letters*, **56**, 188 (2002).

2. R.S. Devan, B.K. Chougle, *Physica* B, **393**, 161 (2007).

3. E.Ateia, M.A.Ahmed, A.K.El-Aziz, J.Magn.Magn.Mater., 311 (2007) 545.

4. A.M. Abo El Ata, M.K.El Nimr, S.M. Attia, D.El Kony, A.H. Al-Hamadani, *J. Magn. Magn. Mater.*, **297**, 33 (2006).

5. T.M.Meaz, S.M. Attia, A.M. Abo El Ata, *J. Magn. Magn. Mater.*, **257**, 296 (2003).

6. J.Smit, H.P.Wijn, "*Ferrites*", Cleaver-Hume Press, London, (1959).

7. A.M. Abo El Ata, M.K. El Nimr, D. El Kony, A.H. AL-Hammadi, *J. Magn. Magn. Mater*., **204**, 36-44 (1999).

8. A.M. Abo El Ata, M.A. El Hiti, *J. Phys*. III (France) **7**, 883 (1997).

9. S.R.Elliott, *Adv. Phys*., **36**, 135 (1987).

10. A.K.Jonscher, "*Dielectric Relaxation in Solids*", Chelsea, Dielectrics Press., London, (1983).

11. A.M.Abo-El Ata, M.A.El Hiti, M.K.El Nimr, *J. Mater. Sci. Letters*., **17**, 409 (1998).

12. M.Kaiser, *J.Alloys and Compounds*, **468**, 15 (2009).

13. M.A.Ahmed, M.A.El Hiti, M.M.Masoad, S.A.Attia, *J. Magn. Magn. Mater*., **146**, 84 (1995).

14. H. M. Zaki, *Physica* B, **363**, 232 (2005).

15. C. G. Coops, *Phys. Rev*., **83**(1), 121 (1951).

16. W.D.Kingery, H.K.Bowen, D.R.Uhlmann, "*Introduction to Ceramics*", 2^{nd} Edn., Wiley-Interscience Pub., (1975).

17. A.A.Zaky and R.Hawley, "Dielectric Solids", London: Routledge & Kegan Paul Ltd., (1970).

18. M.K.Fayek, S.S.Ata-Allah, H.A.Zayed, M.Kaiser, S.M.Ismail, *J. Alloys and Compounds*, **469**, 9 (2009).

19. D. Ravinder, K. Latha, *Mater. Letters*, **41**, 247 (1999).

20. K.M.Batoo, S.Kumar, C.G.Lee, Alimuddin, *Curr. Appl. Phys*., **9**, 1397 (2009).

21. M. K. Fayek, S. S. Ata-Allah, H. A. Zayed, M. Kaiser, S. M. Ismail, *J. Alloys. Comp*., **469**, 9–14 (2009).

22. K. Iwauchi and Y. Ikeda, *Phys. Stat. Sol*., (a) **93**, 309 (1986)

23. A. Goldman, "*Modern Ferrite Technology*", Van Nostrand Reinhold, New York, (1990).